Intercalibration of microwave sounding unit with short overlaps

Cheng-Zhi Zou

Center for Satellite Applications and Research, NOAA/NESDIS, Camp Springs, Maryland, USA

ABSTRACT

NOAA/NESDIS/Center for Satellite Applications and Research has been reprocessing and recalibrating the Microwave Sounding Unit (MSU) observations to generate atmospheric temperature dataset with climate quality. So far, observations from the MSU channels 2, 3, and 4 for NOAA 10, 11, 12, and 14 have been recalibrated using a recently-developed SNO (simultaneously nadir overpasses) sequential nonlinear calibration technique and a 20-year long deep-layer atmospheric temperature dataset from 1987 to 2006 has been generated. However, when using the SNO nonlinear technique to intercalibrate the MSU instrument for satellites before NOAA 10, one has to deal with the short overlap issue for satellites between NOAA 9 and NOAA 10. In this study, by extending the spatial distance criterion for the SNO matchups, we generate more SNO samplings for the short-overlapping satellites. We analyze the error characteristics of the SNO matchups when the spatial distance is extended to as large as 650km. We also generate calibration coefficients using the SNO nonlinear sequential intercalibration technique and then analyze how the intercalibration affects the SNO biases with different separation distances. These analyses will be helpful in determining the final calibration coefficients used for generating consistent MSU long-term temperature time series that will include all available satellites.

Keywords: MSU dataset; MSU atmospheric temperature trend; satellite intercalibration; simultaneous nadir overpasses; satellite merging; warm target contamination; short overlaps.

1. INTRODUCTION

The Microwave Sounding Unit (MSU) on board the NOAA polar-orbiting satellites is uniquely positioned to provide long-term temperature measurement with global coverage that other traditional measurements cannot offer. However, calibration errors are one of the major uncertainties in using the MSU observations for climate trend detection. To reduce these uncertainties and generate climate-quality atmospheric temperature dataset, NOAA/NESDIS has been reprocessing and recalibrating the MSU observations using simultaneous nadir overpasses (SNO) (Zou et al. 2006, 2008). The SNO matchups used for these calibrations contain nadir observations of two overpass satellites within a time interval of 100 seconds and a ground distance of 111 km. So far, observations from the MSU channels 2, 3, and 4 for NOAA 10, 11, 12, and 14 have been recalibrated and a 20-year long deep-layer atmospheric temperature dataset from 1987 to 2006 has been generated for these channels (Zou et al. 2008). However, when using SNO techniques to intercalibrate the MSU instruments for satellites before NOAA 10, it was found that the SNO sampling numbers for NOAA 10 and NOAA 9 overlaps are much lower than the required minimum for the previously specified SNO separation distance and time interval (Zou et al. 2006). Because of this, we suspect that the calibration coefficients obtained from such small SNO samplings would not be accurate enough for instrument calibration purposes. In fact, short overlaps between NOAA-9 and NOAA-10 caused large uncertainties in determination of the MSU atmospheric temperature trend (Mears and Wentz 2005). In this study, by extending the separation distance for the SNO matchups, we generate more SNO samplings for the short-overlapping satellites. We analyze the error characteristics of the SNO datasets when the SNO ground separation distance is extended to as large as 650 km. We also generate calibration coefficients using a SNO nonlinear sequential intercalibration technique developed in our previous study and then analyze how the calibration affects the SNO biases with different separation distance. These analyses will help us to determine the final calibration coefficients used for generating consistent MSU long-term temperature time series that will include all available satellites.

2. PROBLEMS WITH SHORT OVERLAPS

Short overlaps are situations where overlapping observations of two satellites occur only for a relatively short period. Since the frequency of finding the SNO events for two satellites are determined by the

satellite orbital parameters (Cao et al. 2004), only a relatively small number of SNO events can be found for short overlapping satellites. Table 1 is taken from Zou et al. (2006), which shows the overlapping time period for all NOAA polar-orbiting satelites that contain MSU instruments. The table also includes the corresponding SNO smapling numbers when the SNO simoutaneity criteria are set to be 100 seconds for the time interval and 111 km for the ground space distance. Only SNOs for the nadir footprints are shown in the table.

Table 1 Overlapping periods and SNO numbers of the nadir pixels for different overlap NOAA satellites. The time difference is 100 sec and separation distance is 111 km for the criteria of simultaneity (From Zou et al. 2006).

Overlap Satellites	TN-N6	N6-N7	N7-N8	N8-N9	N6-N9	N9-N10	N10-N11	N10-N12	N11-N12	N11-N14	N12-N14
Overlapping Period	01/80-12/80	08/81-12/82	05/83-05/84	07/85-08/85	11/85-10/86	12/86-02/87	10/88-08/91	06/91-08/91	06/91-12/94	08/97-04/98	01/95-11/98
SNO Number	86	329	232	37	217	67	562	470	980	203	1078

As can be seen from Table 1, the SNO samplings for the satellite pairs between TIROS-N (TN) and NOAA 6 (N6), between NOAA-8 and NOAA-9 (N8-N9) and between NOAA 9 and NOAA 10 (N9-N10) are much smaller than the other satellite pairs. This is because these satellite pairs overlap for only 1 to 3 months, much shorter than the other satellite pairs. Note that the overlapping period of NOAA 10 and NOAA 12 (N10-N12) is also short (about 2 months), but their SNO numbers are comparable to the satellite pairs with longer overlapping periods. This occurs because NOAA 10 and NOAA 12 are both morning satellites and at a few times during their overlapping period, their orbits stay close to each other for a relatively longer period so that many SNO data pairs are found for these particular orbits. These SNOs were not used for intercalibration since their spatial distribution is non-random (Zou et al. 2006). Therefore, we will not discuss this set of matchups in the following.

The small SNO sampling numbers for the satellite pairs mentioned above do not satisfy the minimum requirement for satellite intercalibration. This can be understood in the following way. Assuming the SNOs are random samples and we ignore the SNO spatial and time differences. For SNO matchups between satellites *k* and *j*, one computes the brightness temperature (abbreviated as T_b) bias as

$$\text{Bias}=\sum_{i=1}^{N} T_{bi}(k) - T_{bi}(j) \tag{1}$$

where *i* is an index for the SNO numbers, *N* is the total number of the SNO sampling, and *k* and *j* refer to satellites *k* and *j* for the satellite pair. Note this bias is only an estimate of the 'true' bias between satellite *k* and *j* because *N* is a finite number. The error between this bias estimate and the 'true' bias is defined as Ω. For a normal curve test, this Ω is expressed as

$$\Omega = \frac{z_{\eta/2}\sigma}{\sqrt{N}} \tag{2}$$

where σ is the standard deviation of the SNO difference time series, $z_{\eta/2}$ is a confidence coefficient corresponding to the significance level of η. For a 95% confidence (η = 0.05), $z_{\eta/2}$ =1.96.

From Eq. 2, one can derive the minimum sampling requirement for a bias statistics to be significant at the desired level. For the bias statistics such as Eq. (1) to have climate quality, Ω should be less than 0.1K. Assuming a 95% confidence, then the minimum SNO sampling requirement, expressed as N_m, is

$$N_m = \left(\frac{z_{\eta/2}\,\sigma}{\Omega}\right)^2 = \left(\frac{1.96\sigma}{0.1}\right)^2 \tag{3}$$

For the SNO matchups mentioned above (spatial ground distance is 111 km and time interval is 100 seconds), σ = 0.76 K (Zou et al. 2006). This gives the minimum SNO sampling requirement to be 222. From Table 1, we can see that the SNO numbers for satellite pairs TN-N6, N8-N9, and N9–N10, are far below the minimum requirement N_m=222. Thus using these observations for intercalibration may result in lower confidence in the bias statistics and possibly lower quality in the resulting climate dataset.

3. INCREASING SNO SAMPLINGS BY INCREASING SNO SEPARATION DISTANCE

To find more SNO samples, we extend the SNO separation distance to be as large as 650 km with the time interval remains at 100 seconds. To see how the SNO samplings increase with the spatial distance of SNO pixels, Fig. 1 shows a scatter plot of the brightness temperature differences for satellite pairs between NOAA 9 and NOAA 10 versus the nadir pixel distances of the two overpass satellites. The figure clearly show that the number of the SNO points increase substantially when the distance increases from 0 to 220 km. However, when the SNO distance increases, the standard deviation also increases. This feature will affect the bias statistics.

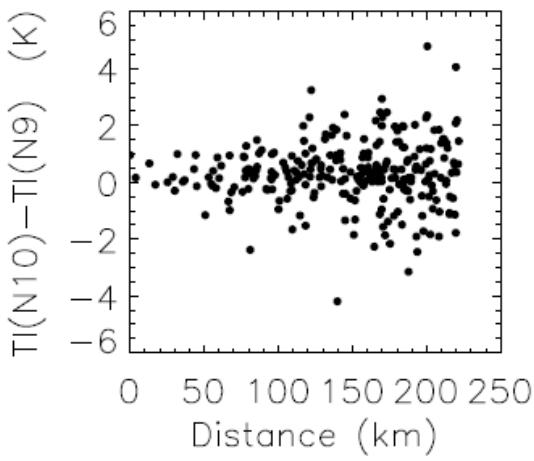

Figure 1 Scatterplot of the brightness temperature difference versus the center distance between two nadir pixels of the overpass satellites for satellite pairs between NOAA 9 and NOAA 10. The time window is set to 100 seconds.

Figure 2 further shows the averaged SNO standard deviation for MSU channel 2 computed for all satellite pairs when the SNO separation distance increases from 20 km to 650 km. The gradual increase of the standard deviation as the SNO separation distance increases reflects the fact that the mid-tropospheric atmosphere has a non-zero temperature gradient.

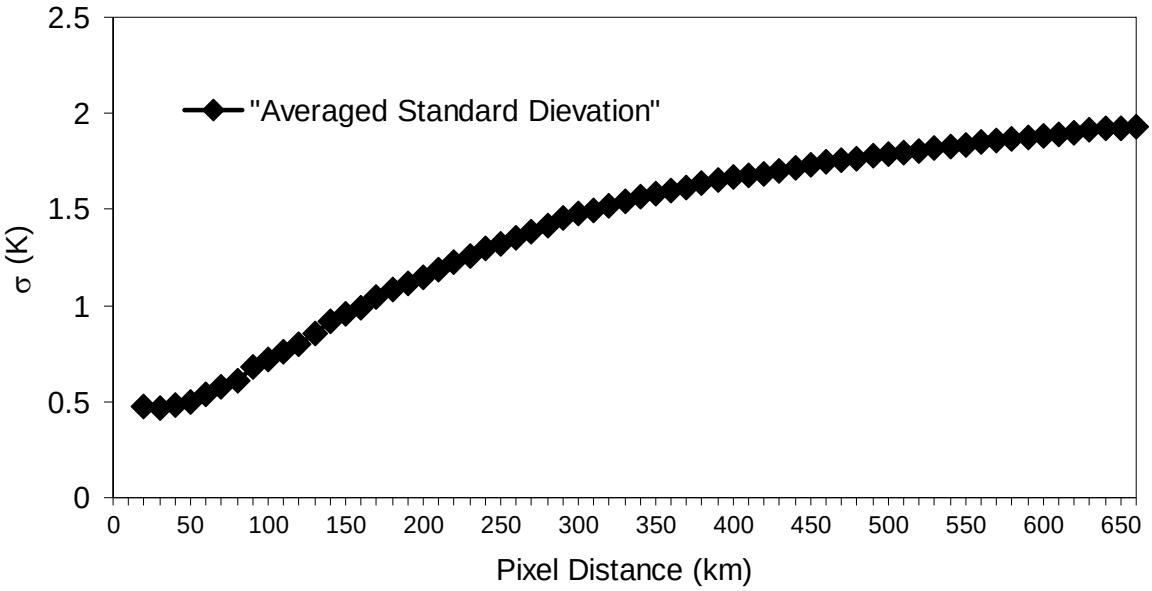

Figure 2 Mean standard deviation (STD) of the MSU channel 2 brightness temperature differences between two satellites versus SNO separation distance of the nadir pixels.

Figure 3 shows the variation of the SNO numbers versus the separation distance of satellite footprints, represented as *d* in the following, of the SNO matchups for satellite pairs with shorter overlapping periods.

The variation of N_m with d is also shown in the plot for a comparison. The N_m is computed using Eq. (3) with the standard deviation shown in Fig. 2 as input. It is seen that when d is small, the SNO sampling numbers are far below the minimum requirement N_m. However, it is also seen that the SNO numbers increase exponentially with d while N_m increases quadratically with d (N_m is proportional to the square of σ while σ increases approximately linearly with d, see Fig. 2). Therefore, when d is large enough, the SNO numbers will eventually catch up with N_m.

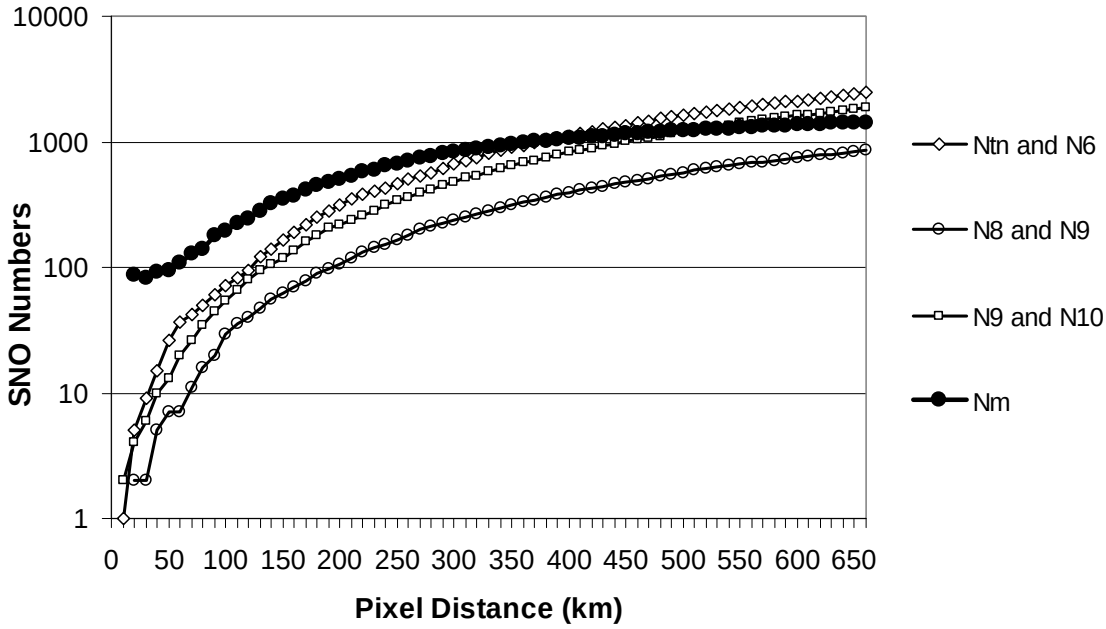

Figure 3 SNO numbers versus SNO separation distance for selected satellite pairs. The thick line 'N_m' represents the minimum sampling requirement.

For the satellite pair TN-N6, the SNO numbers catch up with N_m at d=380 km (SNO number = 1032 for TN-N6 and N_m=1027). Thus at this distance the total SNO number for this satellite pair satisfies the minimum sampling requirement for the bias statistics. For the satellite pair N9-N10, the distance for their SNO numbers to catch up with N_m is 510 km. However, the satellite pair N8-N9 does not satisfy the minimum sampling requirement for the entire distance range (20-650 km) considered in this study. As shown below, these different behaviours of SNO numbers lead to different accuracy in the intercalibration.

In the situation of very large separation distance, the matchups should not be referred to as overpass observations anymore. But here we still use SNO to represent these matchups in the sense that the SNO is an acronym for Simultaneous Nadir Observations.

4. INTERCALIBRATION USING SNO OF DIFFERENT SPATIAL DISTANCES

To use the SNOs to intercalibrate the radiance data, we briefly describe the MSU clibration principles. MSU uses an on-orbit calibration method that includes two calibration targets: the cosmic cold space and an onboard blackbody warm target. The cold space has a temperature of 2.73 K and the warm target temperature is measured by the platinum resistance thermometers embeded in the blackbody target. In each scan cycle, the MSU looks at these targets as well as the earth and the signals from these "looks" are recorded as digital counts. The level 0 calibration converts the digital counts of the earth scene look to the earth scene radiances using the two calibration targets as the end-point references. The calibration equation used here is written as (Zou et al. 2006),

$$R = R_L - \delta R + \mu Z \tag{4}$$

where R is the Earth radiance, $R_L = R_c + S(C_e - C_c)$ represents the dominant linear response and $Z = S^2(C_e - C_c)(C_e - C_w)$ is a nonlinear response; C represents the raw counts and $S = \frac{R_w - R_c}{C_w - C_c}$ is the slope determined by the two calibration points; the subscripts *e, w* and *c* refer to the Earth-view scene, onboard warm blackbody target, and cold space, respectively; δR represents a radiance offset and μ is a nonlinear coefficient. The cold space radiance R_c is specified to be 9.6×10^{-5} mW (sr m^2 cm^{-1})$^{-1}$ for all scan lines. This corresponds to a brightness temperature of 4.78 K that includes the actual cold-space temperature of 2.73 K plus an increase of about 2 K due to the antenna side-lobe radiation. The algorithm for computing R_w can be found in the NOAA Polar Orbiter Data User's Guide. Once the radiance is known, the brightness temperature is computed using the Planck function.

To obtain the calibration coefficients for intercalibration, a radiance error model for the satellite SNO pairs has been established in Zou et al. (2006). The error model for the SNO matchups of satellites *k* and *j* is written as,

$$\Delta R = \Delta R_L - \Delta\delta R + \mu_k Z_k - \mu_j Z_j + E \tag{5}$$

where $\Delta R_L = R_{L,k} - R_{L,j}$ and $\Delta\delta R = \delta R_k - \delta R_j$; E is a residual term and is ignored (see discussion below). In Eq. (5), ΔR_L , Z_k and Z_j are a function of the measurements while $\Delta\delta R$, μ_k and μ_j are unknown coefficients. Regression method is used to solve for these coefficients in which the summation of $(\Delta R)^2$ is minimized. However, since the Z_k and Z_j, terms have a high degree of colieality, only $\Delta\delta R$ and the difference between μ_k and μ_j can be determined from regressions. Therefore, a sequential procedure has been developed in Zou et al. (2006) to obtain the calibration coefficients for satellites from NOAA 10 to NOAA 14. This sequential procedure is also applied here, but now it is used to calibrate satellites from NOAA 10 to TIROS-N. Based on the SNO characteristics, the following path is chosen for the sequential procedure.

First, NOAA-10 is still assumed to be a reference satellite and its offset, δR_{N10}, is assumed to be zero. This assumption will be consistent with previous studies and is easier to connect the previous studies to the satellites before NOAA 10. For a given μ and δR_{N10} =0 for NOAA-10, the calibration coefficients μ and δR for NOAA-9 are obtained from regressions of the SNO matchups between NOAA-10 and NOAA-9 using Eq. (5). After this is done, the coefficients for NOAA-6 are then obtained from the SNO matchups between NOAA-9 and NOAA-6 (see Table 1 for their overlapping). The coefficients for TIROS-N is then obtained from the SNO matchups between TIROS-N and NOAA-6. This is a backward procedure in which older satellites are calibrated sequentially from newer satellites. However, the calibration coefficients for NOAA-7 and NOAA-8 are obtained from a forward process using NOAA-6 as a starting point. In particular, coefficients for NOAA-7 are obtained from SNOs of NOAA-6 and NOAA-7 and then coefficients for NOAA-8 are obtained from SNOs of NOAA-7 and NOAA-8. In this procedure, the SNOs of NOAA-8 and NOAA-9 are not used since they do not satisfy the minimum sampling requirement. This backward and the forward sequential path solves for calibration coefficients for all satellites once the μ and δR for NOAA-10 are known. In our previous study, the NOAA-10 nonlinear coefficient was obtained by requiring the averaged contamination of the warm target temperature in the satellite difference time series to be minimum. This requirement is achieved through a series of sensitivity experiments in which the NOAA-10 nonlinear calibration coefficient was changed from 0 to an arbitrary large number. Here we do not conduct the sensitivity experiments, but simply choose the NOAA-10 nonlinear coefficient obtained from our previous studies as a starting point.

The above described sequential procedure is repeated for all SNO datasets with different separation distance. For each set of SNO matchups, a set of calibration coefficients for all satellites are obtained. These coefficients are then used to compute the radiances for each satellite using Eq. (1). After the brightness temperature is obtained, we compute the SNO T_b biases. To understand how the SNO separation distance (sampling) affects the calibration, Figure 4 shows the SNO bias variation versus the separation distance for some selected set of calibration coefficients. For instance, Figure 4a is the SNO T_b biases when the calibration coefficients obtained from the SNOs of 111 km are applied to compute the SNO T_b for all different separation distance. Only the SNO biases for the satellite pairs N9-N10 and TN-N6 are shown. By definition, we can see that at 111km, the SNO biases for these two satellite pairs are exactly zero in Fig. 4a. However, the calibration coefficients obtained with SNOs of 111 km are not working very well for SNO matchups of other separation distances. This can be seen from the relatively large biases for larger separation distances (on the order of 0.1 for the satellite pair TN-N6 and 0.15 K for the satellite pair N9-N10). The reason for this is that the calibration coefficients obtained from small SNO samplings are not accurate enough for large samplings of SNOs. When using coefficients obtained from SNOs of 150 km and 300 km, the SNO T_b biases for larger separation distances

have been much improved (0.025 K for TN-N6 and 0.05K for N9-N10, Figs. 4b and 4c). Note that the SNO numbers for TN-N6 catch up with the minimum requirement N_m at 380 km. This characteristic appears to be very well reflected by the fact that when the calibration coefficients obtained from the SNOs of 400km (and also of 350 km, but not shown) are used, the biases of the calibrated T_b biases are nearly exactly zero (0.001K) for SNO datasets with larger separation distances (Fig. 4d). For the N9-N10 satellite pairs, the biases are also improved (0.025K) with 400km SNOs, although not to the level of the TN-N6 satellite pair. This is most likely because the SNO numbers at d=400km is still smaller than N_m for the N9-N10 satellite pair.

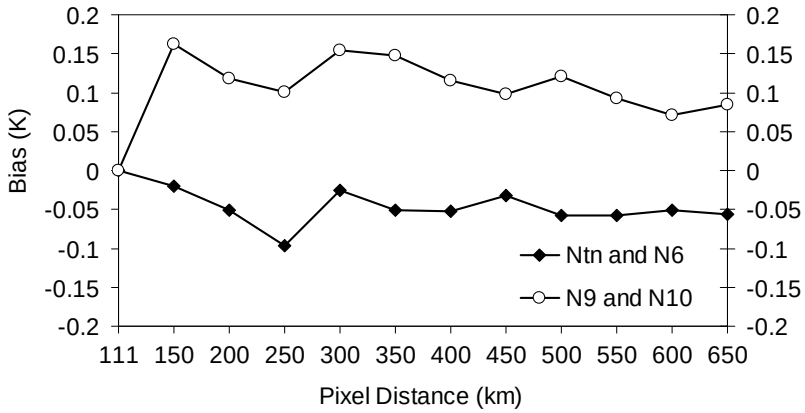

(a) 111 km

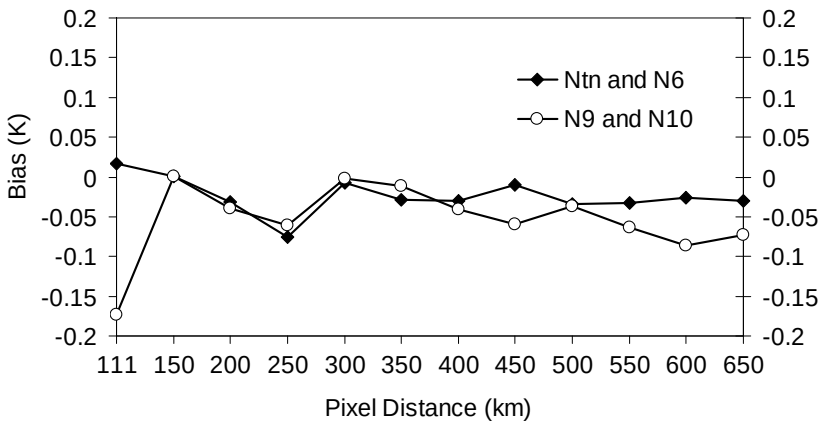

(b) 150 km

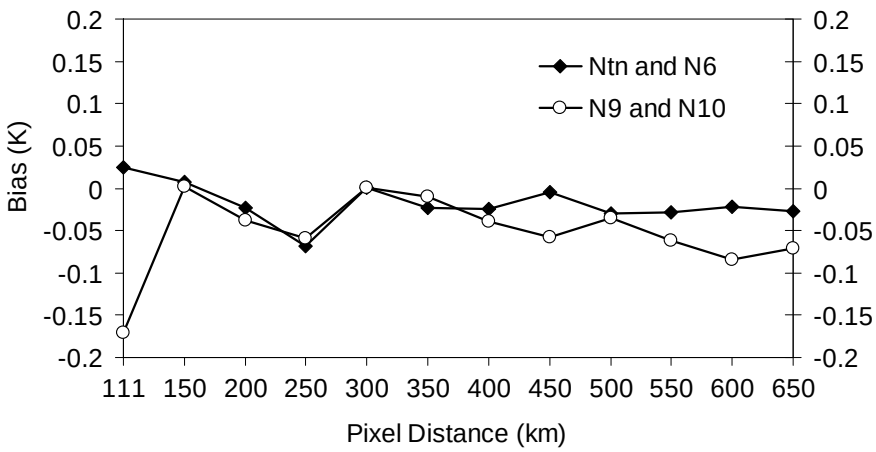

(c) 300 km

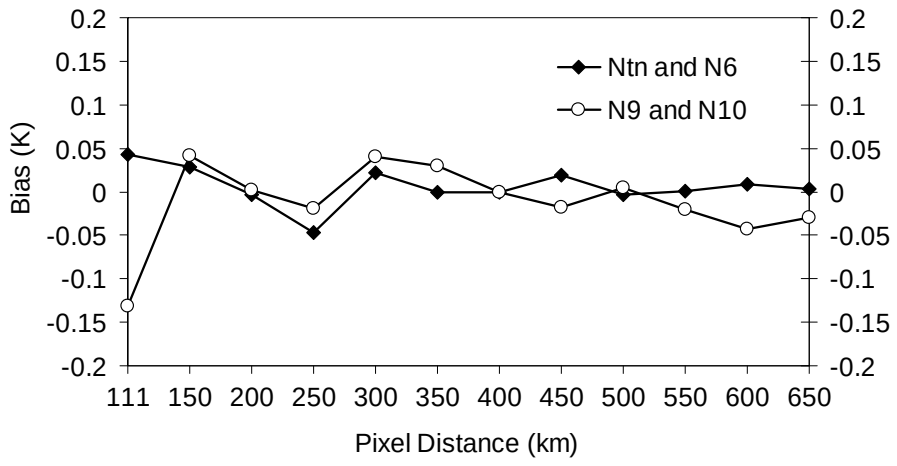

(d) 400 km

Figure 4 T_b biases in the SNO matchups for different pixel separation distance when calibrated using coefficients obtained from the SNO dataset with pixel separation distance of (a) 111km, (b) 150 km, (c) 300km, and (d) 400km.

5. DISCUSSION

The results presented in this study suggest that calibration coefficients obtained from a specific set of SNO samplings can nicely remove intersatellite biases of larger SNO samplings as long as the SNO sampling number for obtaining the calibration coefficients is large enough. This is a nice progress for understanding the robustness of using the SNOs for intercalibration. One issue involved in this investigation is that when the SNO separation distance is very large, the residual term *E* in Eq. (5) should also be large. So in these cases, one shall be cautious to use Eq. (5) for obtaining the calibration coefficients. But from the results presented above, ignoring this term does not appear to affect the SNO biases, i.e., the SNO biases are rather small when the calibration coefficients obtained with SNOs of large separation distance are applied. The reason for this is most likely because the SNO error distribution has spatial symmetric characteristics (Zou et al. 2006). The results shown in Fig. 3 suggest that, although the residual term *E* is large for larger SNO separation distance, we may still ignore this term since the symmetric characteristics may help to cancel out the errors in the regressions so one can still obtain calibration coefficients with reasonable accuracy.

Although the biases are stable for different SNO datasets, the calibration coefficients themselves are different using different SNO datasets (not shown). This may potentially affect the climate trend of the calibrated time series. This problem is still under investigation. We will test how calibration coefficients obtained from different SNO datasets remove warm target contamination and then determine the best separation distance for the calibration.

Acknowledgments. The views, opinions, and findings contained in this report are those of the author(s) and should not be construed as an official National Oceanic and Atmospheric Administration or U.S. Government position, policy, or decision.

References

Cao, C., M. Weinreb, and H. Xu, Predicting simultaneous nadir overpasses among polar-orbiting meteorological satellites for the intersatellite calibration of radiometers, *J. Atmos. Oceanic Technol.*, *21*, 537-542 (2004).

Mears, C. A., and F. J. Wentz, The effect of diurnal correction on the satellite-derived lower tropospheric temperature, *Science*, *309*, 1548-1551 (2005).

NOAA Polar Orbiter Data User's Guide, November 1998 Revision, http://www2.ncdc.noaa.gov/docs/intro.htm.

Zou, C., Goldberg, M., Cheng, Z., Grody, N., Sullivan, J., Cao, C. and Tarpley, D., Recalibration of microwave sounding unit for climate studies using simultaneous nadir overpasses. *J. Geophys. Res.* **111,** D19114: doi: 10.1029/2005JD006798, issn: 0148-0227 (2006).

Zou, C.-Z., M. Gao, and M. Goldberg**,** Error structure and temperature trends in observations from the microwave sounding unit, *J. Climate*, In press, 2008